Chromogenic and Neurotoxic Effects of an Aliphatic γ-Diketone: Computational Insights into the Molecular Structures and Mechanism

Chang-Guo Zhan,[†,‡] Peter S. Spencer,[§] and David A. Dixon*[,†,⊥]

Fundamental Science Directorate, Pacific Northwest National Laboratory, Mailstop K9-90, P.O. Box 999, Richland, Washington 99352, Division of Pharmaceutical Sciences, College of Pharmacy, University of Kentucky, 907 Rose Street, Lexington, Kentucky 40536, and Center for Research on Occupational and Environmental Toxicology, Oregon Health and Sciences University, 3181 South West Sam Jackson Park Road L606, Portland, Oregon 97201

Received: December 4, 2003

First-principles electronic structure calculations have been performed to predict chromogenic properties of various candidate structures, including pyrrole monomers and dimers and their derivatives, of the chromophores formed from the reactions of 2,5-hexanedione (2,5-HD), a prototype of neurotoxic aliphatic γ-diketones, with NH_3, amino acids, and proteins. The calculated results indicate that the pyrrole monomer structures and a previously proposed dimer structure do not have an absorption in the visible region ($\lambda > \sim$400 nm and $< \sim$700 nm), whereas a novel type of pyrrole dimer structure has absorptions ($\lambda = \sim$400 to 420 nm) in the visible region if the methyl (CH_3) groups on the pyrrole rings are oxidized to CHO groups. The calculated results for the oxidized pyrrole dimer models for cross-linked proteins are consistent with all of the available experimental data for the chromogenic and neurotoxic effects of 2,5-HD. Our results strongly support the conclusion that the chromogenic effects of aliphatic γ-diketones are closely related to their neurotoxic effects and further predict that both the chromogenic and neurotoxic effects are associated with the same chemical reaction process. Such a reaction process most likely starts from the formation of the pyrrole−protein adducts followed by dimerization and further oxidization.

Introduction

Aliphatic and aromatic hydrocarbon compounds that can lead to chromogenic/neurotoxic behavior are present in fuels and solvents and, formerly, in consumer products. They have been found in contaminated soil and water at hazardous-waste sites such as the Superfund sites.[1−3] These neurotoxic organic solvents produce chromogenic effects in humans and animals through their oxidation metabolites, γ-diketones. For example, 2,5-hexanedione (2,5-HD), an aliphatic γ-diketone, can be metabolized from *n*-hexane,[4,5] a common aliphatic hydrocarbon solvent that is also present at up to 9% in automotive fuels. *N*-Hexane is used as a solvent in a wide range of processes including ink and paint manufacturing, in the extraction of vegetable oils for use in foods, and as a replacement for benzene in a number of cases. While occupational *n*-hexane neuropathy is now rare in the West, the disease is extant in southern China where the substance continues to be widely employed for its solvent properties.[6]

The γ-diketones themselves are all colorless[7] and, while neurotoxic potencies differ markedly, low potency aliphatic and high potency aromatic γ-diketones display related neurotoxic and chromogenic properties.[8,9] A notable difference exists in the specific color of the chromophore formed from the reaction with proteins/amino acids. For example, 1,2-diacetylbenzene (1,2-DAB), an aromatic γ-diketone, forms blue pigments on contact with proteins, skin, and other tissues.[3,10,11] Rodents treated systemically with 1,2-DAB develop blue discoloration of skin, eyes, and internal organs, including the brain and spinal cord.[10,12−15] The color of the pigment formed from the reactions of aromatic γ-diketones, such as 1,2-DAB, with proteins/amino acids is pH dependent; the pigment displays a blue or violet color in neutral and acidic solutions and it exhibits a brown color at pH ≥7.5.[9,10] However, the pigments formed from the reactions of aliphatic γ-diketones, such as 2,5-HD, with proteins/amino acids are always yellow/brown and do not dramatically change with changing the pH of the solution.[5]

A number of experimental studies have provided insights into the molecular mechanisms of the chromogenic effects of aromatic and aliphatic γ-diketones. Recent experimental studies suggest that aromatic and aliphatic γ-diketones have common neural targets.[9,10] Other reported experimental results and structure−activity considerations led to hypotheses for the possible molecular mechanisms of the chromogenic effects.[5,16,17] However, it is difficult to identify the chromophores by experiment alone because the reaction systems are complicated mixtures and the reaction products have not yet been separated. Therefore, reliable predictions of possible chromophores based on good calculations of their electronic spectra are needed to complement ongoing experimental investigations to uncover the molecular mechanisms of the chromogenic effects.

There have been dramatic changes in computational chemistry over the last two decades. Electronic structure theory has become an effective and powerful tool for use in predicting the properties of a wide range of molecules including geometries, energetics, and spectra (IR/Raman vibrational spectra, NMR, and UV−vis). One of the main reasons for the acceleration of the use of electronic structure theory in predicting molecular properties for larger molecules has been the development of density

† Pacific Northwest National Laboratory.
‡ University of Kentucky (E-mail: zhan@uky.edu).
§ Oregon Health Sciences University.
⊥ Current address: Chemistry Department, The University of Alabama, Box 870336, Tuscaloosa, AL 35487-0336.

10.1021/jp0312868 CCC: $27.50 © 2004 American Chemical Society
Published on Web 04/20/2004

CHART 1

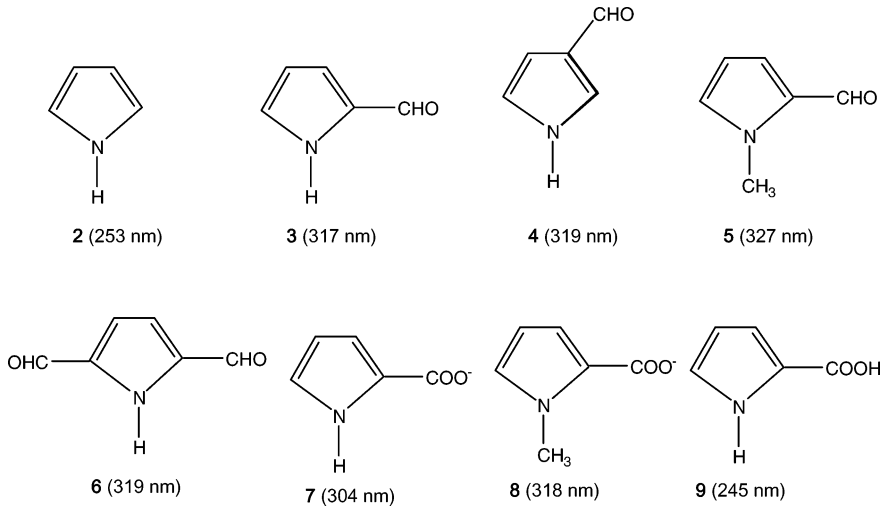

functional theory (DFT).[18−20] The combination of low computational cost with reasonable accuracy has led to the successful application of the DFT method to the prediction of a broad range of properties of molecules in the ground state.[21] In contrast to the case of ground states, time-dependent density functional theory (TD-DFT) for treating excited-state properties[22−24] has only recently been applied to molecules,[25,26] although the theory itself was first proposed more than 20 years ago. Recent work has shown that TD-DFT can be used to reliably predict not only the location of the UV−vis excitation but also the oscillator strength (intensity of the transition).[27,28] In addition, Adamo and Barone[29] have tested TD-DFT calculations in models of aqueous solutions, although the calculated results indicate that the solvent shifts of the calculated excitation energies are small compared to the accuracy required to qualitatively predict the color of a compound.

Our goal is to establish a firm molecular understanding of the chromogenic and neurotoxic effects of both aromatic and aliphatic γ-diketones. For aromatic γ-diketones, we recently reported a series of first-principles electronic structure calculations that were used to predict the chromogenic properties of various candidate structures of the chromophores.[7,30] The calculated results, in a detailed comparison with the previously reported experimental data,[9,10] showed that the oxidized isoindole dimers formed from the reactions of aromatic γ-diketones with proteins/amino acids are a reasonable set of chromophores. Our results support the conclusion that the chromogenic effects of aromatic γ-diketones are closely related to their neurotoxic effects. Both the chromogenic and neurotoxic mechanisms of aromatic γ-diketones are likely associated with the same reaction process, including the formation of the isoindole−protein adducts followed by the dimerization and further oxidization. Through dimerization of the isoindole−protein adducts, aromatic γ-diketones can lead to cross-linking of neurofilament proteins to form colored, high-molecular-weight adducts. This results in the accumulation of neurofilaments in focal swellings within the nerve fiber axon, which is followed by localized demyelination, distal nerve fiber degeneration, and dysfunction in the area of innervation.[30]

Are the molecular mechanisms of the chromogenic and neurotoxic effects of aliphatic γ-diketones similar to those of aromatic γ-diketones? In the present study, we attempt to answer this question to improve our structural and mechanistic understanding of the chromogenic and neurotoxic effects of aliphatic γ-diketones. We focus on 2,5-HD because 2,5-HD is the prototypical aliphatic γ-diketone that shows similar chromogenic and neurotoxic effects.

SCHEME 1

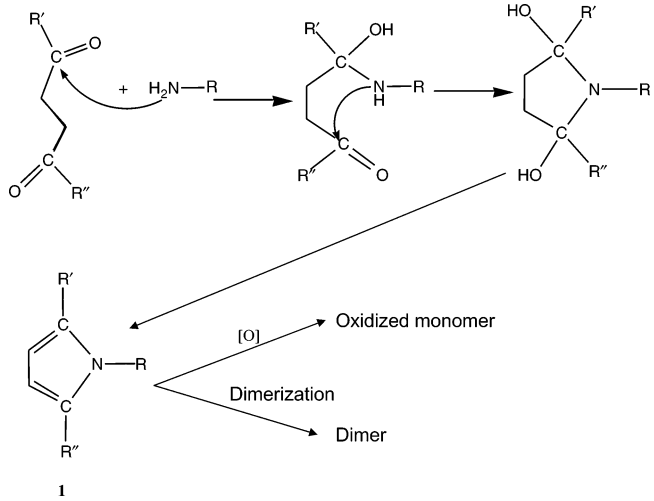

1

A popularly accepted hypothesis[5] for the molecular mechanism of the chromogenic effects of aliphatic γ-diketones, e.g. 2,5-HD, includes the formation of a pyrrole−protein adduct (**1** in Scheme 1). However, it is well-established that pyrrole itself (**2** in Chart 1) and some substituted pyrroles do not absorb in the visible region.[31,32] However, the pyrrole−protein adduct can exhibit color by either subsequent autoxidation[16] or dimerization[5] (Scheme 2). On the basis of the hypotheses described in the literature, the autoxidation of the dimethyl pyrrole−protein adduct formed from 2,5-HD should lead to an adduct structure in which the two methyl groups are all converted into CHO groups,[16] whereas the dimerization of the pyrrole−protein adducts should lead to structure **10** as shown in Scheme 2.[5]

To understand the chromogenic and neurotoxic effects of 2,5-HD at the molecular level, we have employed first-principles electronic structure methods, including DFT and TD-DFT, to predict the structures and colors of various chromophore candidates. The calculations show that both the previously hypothesized pyrrole−protein adduct monomers and pyrrole−protein adduct dimers such as **10** should be colorless. We propose a new dimerization process and show that the observed color could be associated with this process (i.e. from **1** to **11** as shown in Scheme 2) followed by further oxidation (Scheme 3). The calculated results based on this new structural hypothesis

SCHEME 2

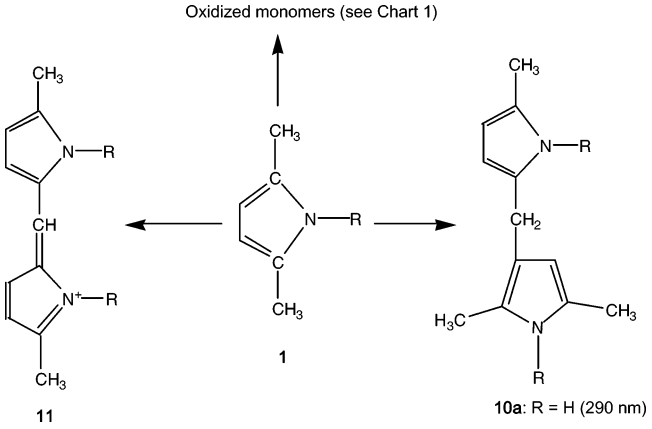

SCHEME 3

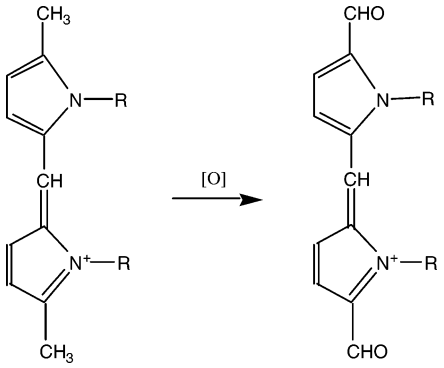

are completely consistent with all of the experimental data for the chromogenic and neurotoxic effects of 2,5-HD.

Computational Methods

Geometries of all species considered in this study were fully optimized by using gradient corrected-DFT with Becke's three-parameter hybrid exchange functional and the Lee−Yang−Parr correlation functional (B3LYP)[33] with the 6-31G(d) basis set.[34] Analytical second-derivative calculations, which yield the harmonic vibrational frequencies, were performed at the optimized geometries to ensure that the optimized geometries are minima on the potential energy hypersurface (all real frequencies). The geometries optimized at the B3LYP/6-31G(d) level were further refined at the B3LYP/6-31+G(d) level of theory. Our previous computational studies[7] show that geometry optimizations at the B3LYP/6-31G(d) and B3LYP/6-31+G(d) levels are sufficiently accurate for these predictions; the use of geometries optimized with larger basis sets should not significantly change the finally calculated energetic and spectral results. The geometries optimized at the B3LYP/6-31+G(d) level were used in time-dependent DFT (i.e. TD-DFT)[35] calculations with the B3LYP functional and the 6-31G(d) basis set augmented with a set of Rydberg functions (3s3p3d) centered at the molecular mass center (mc)[36] to calculate the energies of the singlet vertical transitions. The Gaussian exponents of this set of Rydberg functions are 0.005858 (3s), 0.003346 (4s), 0.002048 (5s), 0.009988 (3p), 0.005689 (4p), 0.003476 (5p), 0.014204 (3d), 0.008077 (4d), and 0.004927 (5d). This set of Rydberg functions has been used in recently reported calculations of the electronic excitations in pyrrole.[36,37] For convenience, this extended basis set is denoted by 6-31G(d)+Ryd(mc). Some TD-DFT calculations were also performed at the B3LYP/6-31+G* level. In addition, a larger basis set, aug-cc-pVTZ,[38] was also

SCHEME 4

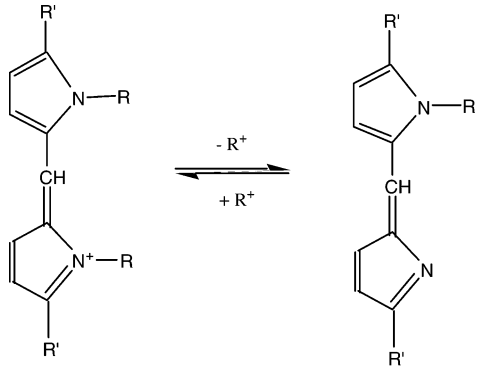

11a	R = H, R′ = H	**12a**
11b	R = CH_3, R′ = H	**12b**
11c	R = CH_3, R′ = CH_3	**12c**
11d	R = H, R′ = CHO	**12d**
11e	R = CH_3, R′ = CHO	**12e**

used in some of the energy calculations (see below). All of the TD-DFT calculations were performed in the gas phase.

To estimate the thermodynamic equilibration between the two pyrrole dimer structures **11a** and **12a** (Scheme 4) in aqueous solution, the geometries optimized at the B3LYP/6-31+G(d) level in the gas phase were used in self-consistent reaction field (SCRF) calculations at the HF/6-31+G(d) level to calculate the free energies of solvation in aqueous solution. The calculated free energy in solution was taken as the free energy calculated at various levels in the gas phase with the B3LYP/6-31+G(d) zero-point vibration and thermal energy corrections plus the solvent shift calculated at the HF/6-31+G(d) level. The present SCRF method was developed and implemented recently in a local version of the GAMESS program[39] by one of us, and is called the surface and volume polarizations for electrostatic interaction (SVPE) model.[40] The SVPE model is also known as the fully polarizable continuum model (FPCM)[41,42] because it fully accounts for both surface and volume polarization effects in the SCRF calculation through an efficient three-dimensional integration algorithm.[40a] Since the solute cavity surface is defined as a solute electron charge isodensity contour determined self-consistently during the SVPE iteration process, the SVPE results, converged to the exact solution of Poisson's equation with a given numerical tolerance, depend only on the contour value at a given dielectric constant and a certain quantum chemical calculation level.[40a] This single parameter value has been determined to be 0.001 au based on an extensive calibration study.[30b] The SVPE procedure using the 0.001 au contour has been shown to be reliable for predicting the free energy of solvation and the pK_a in other biologically interesting systems.[30,41] Previous pK_a calculations[7] on other similar molecules also indicate that using geometries optimized in solution, instead of those in the gas phase, does not significantly change the results. The dielectric constant of water used for the solvation calculations is 78.5. The free energy of solvation of the proton has recently been reliably determined by a supermolecule-continuum approach and this value is used in the current study.[42]

Geometry optimizations and energy evaluations in the gas phase were performed by use of the Gaussian98 program.[43] A local version[40a] of the GAMESS program[39] was used to perform the SVPE calculations. The current version of the SVPE implementation[40a] has its own limitations. In particular, the current SVPE implementation is not capable of performing geometry optimization and calculation of the vertical excitation

energy in solution. Solvent shifts of the excitation energies were estimated by carrying out TD-DFT calculations at the B3LYP/6-31+G* level, using the integral equation formalism for the polarizable continuum model (IEFPCM).[44−48] It has recently been shown[44] through a comparison with Chipman's work[49] on the surface simulation of volume polarization effects that the IEFPCM formulation actually includes a reasonable surface simulation of volume polarization effects when the charge renormalization scheme is ignored. The solute cavity used in the IEFPCM method is defined as interlocked van der Waals spheres centered at solute nuclei. The default standard parameters associated with the united atom topological model (UATM)[50] in the Gaussian03 program[51] were used in our IEFPCM calculations. All calculations were performed on an SGI Origin 2000 computer.

Results and Discussion

Molecular structures considered in this study are shown in Chart 1 and Schemes 2−4. In Chart 1, structures **3**−**9** represent the simplified models of the possible products of the autoxidation of pyrrole−protein/amino acid adduct monomers. **10** to **12** in Schemes 2 and 4 are all the hypothesized dimer structures. The stable framework structures of the pyrrole monomers **2**−**9** are all planar. The framework structures of dimers **11** and **12** also tend to be planar, favoring an extended, conjugated π-bonding system, but only those of **12** are perfectly planar. Although the framework structures of **11** all slightly deviate from planarity due to steric resistance between the two bulk groups (R), the extended, conjugated π-bonding systems are approximately maintained. The substituted pyrrole dimer **10** is nonplanar because the two pyrrole rings cannot form an extended, conjugated π-bonding system. (The molecular coordinates are given as Supporting Information as are the total energies.)

Molecules **11a/11d** and **12a/12d** are the potential protonated and deprotonated products of the reaction of **1** with an amine, modeled in this case by ammonia (NH_3) for which R = H. The other substituted pyrrole dimers all refer to the model structures of possible products of the reactions of the aliphatic γ-diketones with free amino acids or amino acid residues of proteins. In our calculations, we only used R = H or CH_3.

To estimate the thermodynamic equilibration between the deprotonated and protonated states of the products of the reaction of aliphatic γ-diketone with NH_3, we calculated the pK_a for the deprotonation process **11a** → **12a** + H^+ by performing first-principles calculations on the gas-phase geometries of **11a** and **12a**, using the B3LYP functional with a sufficiently large basis set, aug-cc-pVTZ, for the gas-phase electronic energy differences, and using the SVPE method at the HF/6-31+G(d) level for the solvation free energies. Our previous calculations on the pK_a of the similar compounds indicate that the aug-cc-pVTZ basis set is sufficient for the gas-phase electronic energy calculations, whereas a smaller basis set like 6-31+G(d) is adequate for evaluating the solvent shift.[7,30]

It is also necessary for the prediction of the absolute pK_a to know the absolute free energy of the proton in aqueous solution. We recently calculated the absolute hydration free energy of the proton, $\Delta G_{hyd}^{298}(H^+)$, by using a high-level, ab initio method of incorporating a hybrid supermolecule-continuum approach based on the same SVPE procedure used in the present study. $\Delta G_{hyd}^{298}(H^+)$ was predicted[42] to be −262.4 kcal/mol in good agreement with the most recently reported "experimental" value of −264.1 kcal/mol from cluster extrapolations[52] and other theoretical values.[53] The free energy change for the deprotonation process **11a** → **12a** + H^+ in the gas phase is calculated as 226.5 kcal/mol (gas-phase basicity). Including the absolute solvation free energies of all species, the free energy change (ΔG_{sol}) for the deprotonation process **11a** → **12a** + H^+ in aqueous solution is predicted to be 5.6 kcal/mol. The corresponding pK_a is calculated as p$K_a = \Delta G_{sol}/(2.303RT) = 4.1$ at $T = 298$ K. A value of p$K_a \approx 4.1$ indicates that when the pH value is about 4.1, the concentrations of the deprotonated and protonated structures should be equal to each other. At lower pH, the protonated structure should be dominant, whereas at higher pH the deprotonated structure should be dominant.

TABLE 1: Electronic Excitations (λ in nm) and Oscillator Strengths (f) Calculated by Using the TD-DFT Method at the B3LYP/6-31G(d)+Ryd(mc) Level for Various Pyrrole Dimers[a]

substituents in pyrrole dimer			gas phase		aq soln[d]	
R	R′		λ^b	f^b	λ^b	f^b
H	H	**11a**	360 (366)	0.6328 (0.6534)		
CH_3	H	**11b**	378	0.4323		
CH_3	CH_3	**11c**	385	0.7265		
H	CHO	**11d**	497 (493)	0.0000 (0.0000)[c]	(424)	(0.0000)[c]
			496 (491)	0.0017 (0.0003)[c]	(423)	(0.0086)[c]
			404 (412)	0.6773 (0.6751)	(442)	(0.7823)
			363 (366)	0.0867 (0.0788)	(382)	(0.0477)
CH_3	CHO	**11e**	524	0.0000[c]		
			520	0.0004[c]		
			417	0.5876		
			399	0.0206		
H	H	**12a**	363 (372)	0.3387 (0.4145)		
H	CHO	**12d**	453 (447)	0.0000 (0.0000)[c]	(398)	(0.0000)[c]
			412 (420)	0.2624 (0.3156)	(444)	(0.5825)
			398 (396)	0.0000 (0.0001)[c]	(376)	(0.0001)[c]
			386 (391)	0.4111 (0.3550)	(399)	(0.1743)
CH_3	CHO	**12e**	448	0.0001[c]		
			401	0.0360		
			393	0.0010[c]		
			381	0.8480		

[a] Unless indicated, all of the electronic excitations listed are calculated to be $\pi \rightarrow \pi^*$ transitions. [b] The values in parentheses were obtained from TD-DFT calculations at the B3LYP/6-31+G(d) level. [c] These excitations are calculated to be σ (lone pairs on O) → π^* transitions. [d] TD-DFT IEFPCM calculation at the B3LYP/6-31+G* level.

Electronic Excitations. We will first discuss the calculated results for the excitation spectra in the gas phase. We evaluated the electronic excitation energies by performing TD-DFT calculations at the B3LYP/6-31+G(d) and/or B3LYP/6-31G(d)+Ryd(mc) levels. Our previous computational studies[7] of other molecules including an isoindole ring indicate that the electronic excitation energies determined by the TD-DFT calculations are very close to those determined by more sophisticated complete active space multiconfiguration self-consistent field (CASSCF) calculations followed by second-order Møller−Plesset (MP2) perturbations on the multiconfigurational reference states (CAS-MP2).[54] Both the TD-DFT and CAS-MP2 results[7] are in excellent agreement with the available experimental data. Our previous computational studies[7,30] also indicate that both the 6-31+G(d) and B3LYP/6-31G(d)+Ryd(mc) basis sets are sufficient for the TD-DFT calculations; using larger basis sets does not significantly improve the calculated results. As shown in Table 1 for **11a, 11d**, **12a**, and **12d** the TD-DFT transitions calculated at the B3LYP/6-31+G(d) level are close to the corresponding transitions calculated at the B3LYP/6-31G(d)+Ryd(mc) level. The differences in the predicted wavelength for the two basis sets are all within a few nanometers. The wavelengths corresponding to the first excita-

tion energies calculated for **2**−**10** at the B3LYP/6-31+G(d) level are shown in Chart 1 or Scheme 2. The results calculated for **11** and **12** (Scheme 4) are listed in Table 1. For molecules with more than one predicted absorption feature in the visible region, we list in Table 1 the wavelengths of the absorptions corresponding to the first four electronic excitations.

For the first electronic excitation of pyrrole (**2** in Chart 1), our calculated wavelength, 253 nm (4.89 eV), is ∼15 nm longer than the corresponding experimental value, ∼238 nm (∼5.22 eV),[31] suggesting that our TD-DFT calculations slightly underestimate the electronic excitation energies (slightly overestimate the corresponding wavelengths of the absorptions for these molecules).

The results in Chart 1 also show that the first absorption does not significantly change when the H on the N is replaced by a CH_3 group. The molecules in Chart 1 are models of the possible pyrrole−protein/amino acid adduct monomers formed from 2,5-HD. Xu et al.[16] observed that 2,5-HD-derived pyrroles underwent autoxidation at pH 7.4 and that the methyl group (CH_3) on the pyrrole ring could easily be oxidized to become CHO. As shown in Chart 1, our TD-DFT results suggest that linking one or two CHO (or COO^-) groups to the pyrrole ring slightly increases the wavelength of the first absorption, but not by enough to shift the absorption to the visible region. Thus, the pyrrole monomers should not exhibit a color and the chromophore involved in the chromogenic effects of 2,5-HD cannot be a pyrrole monomer.

Molecule**10a** in Scheme 2 is a model of the pyrrole−protein/amino acid adduct dimer hypothesized in the literature.[5] However, our TD-DFT calculations show that the first absorption (290 nm) of **10a** does not dramatically differ from that of the corresponding monomer. This is not surprising, because the two pyrrole rings in **10a** are bridged by a CH_2 group so that an extended, conjugated π-bonding system cannot form. The previously hypothesized dimer structures such as **10a** also will not exhibit a color and are inappropriate candidates for the chromophore involved in the chromogenic effects of 2,5-HD.

We considered the possibility of pyrrole dimer structures, such as **11** in Scheme 2, in light of our recently reported computational studies on the chromogenic and neurotoxic effects of 1,2-DAB.[30] The combination of the new hypothesis with Xu et al.'s observation[16] that a methyl group on the pyrrole ring can easily be oxidized to become a CHO led us to consider the similar oxidation of **11** as shown in Scheme 3. The specific structures such as **11** (**11a** to **11e**) that we calculated are depicted in Scheme 4. As shown in Table 1, the wavelengths of the absorptions corresponding to the first excitation energies of **11a** to **11c** are significantly longer than those of the corresponding monomers due to the formation of an extended, conjugated π-bonding system, and are very close to the visible region (∼400 to 700 nm). The further oxidation shown in Scheme 3, i.e. changing CH_3 into CHO (**11d** and **11e**), makes this novel type of pyrrole dimer colored.

In addition to the structures based on **11**, we also considered a slightly different type of structure as shown in **12**. We note that only structures **12a** and **12d**, the deprotonated forms of **11a** and **11d**, respectively, are likely to be important because the structures based on **11** are thought to be the direct products of the reaction of **1** with ammonia (NH_3) for which R = H. Whether structures based on **12** can be produced or not when R ≠ H will need to be addressed by experiments. It is interesting to note that the color of a structure based on **12** should be similar to that of the corresponding structure based on **11**, because all of the strong absorptions are predicted to be associated with $\pi \rightarrow \pi^*$ transitions. For example, the color of **11d** or **11e** is dominated by a strong absorption at ∼404 or ∼417 nm corresponding to the third electronic excitation, whereas the color of **12d** or **12e** is dominated by a strong absorption at ∼412 or ∼401 nm corresponding to the second excitation. The color of the dominant absorption (∼400 to 420 nm) for **11d** or **11e** and **12d** or **12e** should be close to violet (∼420 nm).[55] Since the complementary color of violet is yellow,[56] the corresponding color of the nonabsorbed light should be close to yellow and this color should not dramatically change with changing the pH of the solution. The results obtained for the aliphatic γ-diketone are in contrast with those obtained previously for the aromatic γ-diketone, where the color of the predicted chromophore is pH dependent (i.e. violet/blue in neutral/acidic solution and brown in basic solution).[30] The predicted yellow color of **11d** or **11e** and **12d** or **12e** is completely consistent with the reported yellow/brown color observed in the chromogenic effects of 2,5-HD.[5,9]

The above discussion of the colors of the various proposed species is based on the TD-DFT results calculated in the gas phase. Solvent and protein environment effects have been ignored. Because the γ-diketones can only react with amino acid residues on the surface of a protein in aqueous solution, we approximate the environment of the reaction products to be that of the aqueous solvent and not dependent on the detailed protein structure. The available experimental studies[9,10] do not show obvious differences between the colors of the chromophore formed from reactions with different proteins. As shown in Table 1, the solvent shifts of the electronic excitations calculated with the IEFPCM method for **11d** and **12d** in aqueous solution are significant, particularly for the σ (lone pairs on O) $\rightarrow \pi^*$ transitions with negligible *f* values. The solvent shifts for these transitions are about 70 nm (∼0.40 eV) to the blue for **11d** and about 50 nm (∼0.34 eV) for **12d**. The intense $\pi \rightarrow \pi^*$ transitions with large *f* values are shifted to the red and the calculated solvent shift for the most intense transition is ∼40 nm (∼0.20 eV) for both **11d** and **12d**. In fact, for both **11d** and **12d**, the most intense transition is now the lowest energy one after being corrected for solvent effects. The calculated solvent shifts are certainly significant, but the dominant absorptions, those with the largest *f* values, shift somewhat to the red but not enough to significantly change the color of the solution. Thus, the solvent and protein environment effects will not qualitatively change the conclusions reached based on the gas-phase calculations.

Relationship between the Chromogenic and Neurotoxic Properties. Although both **11e** and **12e** could be reasonable model structures of possible chromophores in the chromogenic effects of 2,5-HD, only structures based on **11** should be correlated with the neurotoxic effects because only structures based on **11** can potentially be a model for cross-linked proteins. The direct product of the dimerization of **1** can only be a structure based on **11**. To transform **11** into the corresponding structure based on **12** when R ≠ H requires a dealkylation process as compared to a deprotonation process. Compared to the model compounds **11d** and **11e**, the actual structure of the further oxidized pyrrole dimer formed from the reaction of **1** with amino acids (such as lysine) or proteins differs in R where R is such that $R-NH_2$ (or $R-NH_3^+$) represents an amino acid, polypeptide, or protein. In the case of proteins, the dimerization of the formed pyrrole−protein adducts leads to cross-linking between the two proteins, similar to our previously predicted isoindole−protein adduct dimers[30] (formed from the aromatic γ-diketones) that can also cross-link two proteins. This is

consistent with the experimental observation[9] that both aromatic and aliphatic γ-diketones, including **1**, cross-link neurofilament proteins to form higher molecular weight products. The cross-linked neurofilaments accumulate in focal axonal swellings, which appear proximally and distally in systemic aromatic and aliphatic γ-diketone toxicity, respectively. Our results strongly support the conclusion that the chromogenic effects of aliphatic γ-diketones are also closely related to their neurotoxic effects.[9] We further predict that both the chromogenic and neurotoxic effects are likely to be associated with the same reaction process, which probably starts from the formation of the pyrrole−protein adducts followed by the dimerization and further oxidization. We note that there is a stepwise increase in neurotoxic potency as methyl groups are added to the backbone of 2,5-HD in the order 2,5-HD < 3-methyl-2,5-HD < 3,4-dimethyl-2,5-HD.[14] Understanding this change in neurotoxic potency as represented by changes in the location of focal swellings within the nerve fiber axon will be the focus of future work.

Conclusion

We have performed a series of first-principles electronic structure calculations to predict the chromogenic properties of various candidate molecular frameworks, including pyrrole monomers and dimers and their derivatives, of the chromophores formed from the reactions of 2,5-hexanedione (2,5-HD), the prototypical neurotoxic aliphatic γ-diketone, with NH_3, amino acids, and proteins. The calculated results predict that the pyrrole monomer structures and a previously proposed dimer structure do not have an absorption in the visible region ($\lambda > \sim$400 nm and $< \sim$700 nm), whereas a pyrrole dimer structure with the methyl groups on the pyrrole rings all oxidized to CHO groups have absorptions ($\lambda = \sim$400 to 420 nm) in the visible region. The calculated results for the oxidized pyrrole dimer models for cross-linked proteins are consistent with all of the available experimental data for the chromogenic and neurotoxic effects of 2,5-HD. Our results support the conclusion that the chromogenic effects of aliphatic γ-diketones are closely related to their neurotoxic effects, similar to the case of aromatic γ-diketones. Both the chromogenic and neurotoxic mechanisms are likely to be associated with the same reaction process, including the formation of the pyrrole−protein adducts followed by dimerization and further oxidization. Further biological and biochemical experiments as well as NMR measurements would be of real value in confirming the identity of the critcal chromogenic and neurotoxic species.

Acknowledgment. This research was performed in part in the William R. Wiley Environmental Molecular Sciences Laboratory (EMSL) at the PNNL. The EMSL is a national user facility funded by the Office of Biological and Environmental Research in the U.S. Department of Energy. PNNL is a multiprogram national laboratory operated by Battelle Memorial Institute for the U.S. Department of Energy. Additional calculations were performed in the Zhan laboratory at the University of Kentucky. The work was funded in part by a subcontract from Oregon Health Sciences University under the auspices of a NIH/NIEHS Superfund Basic Research Center grant # 5 P42 ES 10338.

Supporting Information Available: Geometries and total energies of the pyrrole dimer structures optimized at the B3LYP/6-31+G(d) level. This material is available free of charge via the Internet at http://pubs.acs.org.

References and Notes

(1) Johnson, B. L.; DeRosa, C. T. *Rev. Environ. Health* **1997**, *12*, 235.
(2) Spencer, P. S.; Sterman, A. B.; Horoupian, D. S.; Folds, M. N. *Science* **1979**, *204*, 633.
(3) Spencer, P. S.; Folds, M. N.; Sterman, A. B.; Horoupian, D. S. In *Experimental and Clinical Neurotoxicology*; Spencer, P. S., Schaumburg, H. H., Eds.; Williams and Wilkins: Baltimore, MD, 1980; p 296.
(4) Spencer, P. S.; Schaumburg, H. H.; Sabri, M. I.; Veronesi, B. *Crit. Rev. Toxicol.* **1980**, *7*, 279.
(5) DeCaprio, A. P. In *Experimental and Clinical Neurotoxicology*, 2nd ed.; Spencer, P. S., Schaumburg, H. H., Eds.; Oxford University Press: New York, 2000; p 633.
(6) Spencer, P. S. Personal observation.
(7) Zhan, C.-G.; Dixon, D. A.; Sabri, M. I.; Kim, M.-S.; Spencer, P. S. *J. Am. Chem. Soc.* **2002**, *124*, 2744.
(8) Spencer, P. S.; Kim, M. S.; Sabri, M. I. *Int. J. Hyg. Environ. Health* **2002**, *205*, 131.
(9) Kim, M. S.; Hashemi, S. B.; Spencer, P. S.; Sabri, M. I. *Toxicol. Appl. Pharmacol.* **2002**, *183*, 55.
(10) Kim, M. S.; Sabri, M. I.; Miller, V. H.; Kayton, R. J.; Dixon, D. A.; Spencer, P. S. *Toxicol. Appl. Pharmacol.* **2001**, *177*, 121.
(11) Sabri, M. I.; Hashemi, S.; Kim, M. S.; Spencer, P. S. *J. Neurochem.* **2002**, *81*, 103.
(12) Gagnaire, F.; Marignac, B.; de Ceaurriz, J. *J. Appl. Toxicol.* **1990**, *10*, 105.
(13) Gagnaire, F.; Ensminger, A.; Marignac, B.; de Ceaurriz, J. *J. Appl. Toxicol.* **1991**, *11*, 261.
(14) Spencer, P. S. In *Experimental and Clinical Neurotoxicology*, 2nd ed.; Spencer, P. S., Schaumburg, H. H., Eds.; Oxford University Press: New York, 2000; p 112.
(15) Kim, M. S.; Kayton, R.; Muñiz, J.; Austin, D. R.; Spencer; P. S.; Sabri, M. *Microsc. Microanal.* **1999**, *5* (Suppl. 2), 1218.
(16) Xu, G.; Singh, M. P.; Gopal, D.; Sayre, L. M. *Chem. Res. Toxicol.* **2001**, *14*, 264.
(17) Xu, G.; Sayre, L. M. *J. Org. Chem.* **2002**, *67*, 3007.
(18) Hohenberg, P.; Kohn, W. *Phys. Rev. B* **1964**, *136*, 864.
(19) Kohn, W.; Sham, L. J. *Phys. Rev. A* **1965**, *140*, 1133.
(20) Parr, R. G.; Yang W. *Density-Functional Theory of Atoms and Molecules*; Oxford University Press: Oxford, UK, 1989.
(21) *Recent Advances in Density Functional Methods, Part 1*; Chong, D. P., Ed.; World Scientific: Singapore, 1995.
(22) Ando, T. *Z. Phys. B* **1977**, *26*, 263.
(23) Zangwill, A.; Soven, P. *Phys. Rev. A* **1980**, *21*, 1561.
(24) Runge, E.; Gross, E. K. U. *Phys. Rev. Lett.* **1984**, *52*, 997.
(25) Bauernschmitt, R.; Ahlrichs, R. *Chem. Phys. Lett.* **1996**, *256*, 454.
(26) Casida, M. E.; Jamorski, C.; Casida, K. C.; Salahub, D. R. *J. Chem. Phys.* **1998**, *108*, 4439.
(27) Casida, M. E.; Salahub, D. R. *J. Chem. Phys.* **2000**, *113*, 8918.
(28) (a) Matsuzawa, N. N.; Ishitani, A.; Dixon, D. A.; Uda, T. *J. Phys. Chem. A* **2001**, *105*, 4953. (b) Dixon, D. A.; Matsuzawa, N. N.; Ishitani, A.; Uda, T. *Phys. Status Solidi B* **2001**, *226*, 69. (c) Matsuzawa, N. N.; Ishitani, A.; Zhang, C.-G.; Dixon, D. A.; Uda T. *J. Fluorine Chem.* **2003**, *122*, 27.
(29) Adamo, C.; Barone, V. *Chem. Phys. Lett.* **2000**, *330*, 152.
(30) Zhan, C.-G.; Spencer, P. S.; Dixon, D. A. *J. Phys. Chem. B* **2003**, *107*, 2853.
(31) (a) Mullen, P. A.; Orloff, M. K. *J. Chem. Phys.* **1969**, *51*, 2276. (b) Bavia, M.; Bertinelli, F.; Taliani, C.; Zauli, C. *Mol. Phys.* **1976**, *31*, 479. (c) Flicker, W. M.; Mosher, O. A.; Kuppermann, A. *Chem. Phys. Lett.* **1976**, *38*, 489. (d) Palmer, M. H.; Walker, I. C.; Ballard, C. C.; Guest, M. F. *Chem. Phys.* **1995**, *192*, 111. (e) Palmer, M. H.; Walker, I. C.; Guest, M. F. *Chem. Phys.* **1998**, *238*, 179.
(32) Zhan, C.-G.; Dixon, D. A. *J. Mol. Spectrosc.* **2002**, *216*, 81.
(33) (a) Becke, A. D. *J. Chem. Phys.* **1993**, *98*, 5648. (b) Lee, C.; Yang, W.; Parr, R. G. *Phys. Rev. B* **1988**, *37*, 785. (c) Stephens, P. J.; Devlin, F. J.; Chabalowski, C. F.; Frisch, M. J. *J. Phys. Chem.* **1994**, *98*, 11623.
(34) Hehre, W. J.; Radom, L.; Schleyer, P. v. R.; Pople, J. A. *Ab Initio Molecular Orbital Theory*; John Wiley & Sons: New York, 1986.
(35) Stratmann, R. E.; Scuseria, G. E.; Frisch, M. J. *J. Chem. Phys.* **1998**, *109*, 8218.
(36) Kaufmann, T. H.; Baumeister, W.; Jungen, M. *J. Phys. B* **1989**, *22*, 2223.
(37) Wan, J.; Meller, J.; Hada, M.; Ehara, M.; Nakatsuji, H. *J. Chem. Phys.* **2000**, *113*, 7853 and references therein.
(38) Kendall, R. A.; Dunning, T. H., Jr.; Harrison, R. J. *J. Chem. Phys.* **1992**, *96*, 6796.
(39) Schmidt, M. W.; Baldridge, K. K.; Boatz, J. A.; Elbert, S. T.; Gordon, M. S.; Jensen, J. H.; Koseki, S.; Matsunaga, N.; Nguyen, K. A.; Su, S. J.; Windus, T. L.; Dupuis, M.; Montgomery, J. A. *J. Comput. Chem.* **1993**, *14*, 1347.
(40) (a) Zhan, C.-G.; Bentley, J.; Chipman, D. M. *J. Chem. Phys.* **1998**, *108*, 177. (b) Zhan, C.-G.; Chipman, D. M. *J. Chem. Phys.* **1998**, *109*, 10543. (c) Zhan, C.-G.; Chipman, D. M. *J. Chem. Phys.* **1999**, *110*, 1611. (d) Zhan, C.-G.; Landry, D. W.; Ornstein, R. L. *J. Phys. Chem. A* **2000**, *104*, 7672.
(41) (a) Zhan, C.-G.; Norberto de Souza, O.; Rittenhouse, R.; Ornstein, R. L. *J. Am. Chem. Soc.* **1999**, *121*, 7279. (b) Zhan, C.-G.; Niu, S.; Ornstein, R. L. *J. Chem. Soc., Perkin Trans. 2* **2001**, *1*, 23. (c) Zheng, F.; Zhan,

C.-G.; Ornstein, R. L. *J. Chem. Soc., Perkin Trans. 2* **2001**, 2355. (d) Zheng, F.; Zhan, C.-G.; Ornstein, R. L. *J. Phys. Chem. B* **2002**, *106*, 717. (e) Zhan, C.-G.; Landry, D. W.; Ornstein, R. L. *J. Am. Chem. Soc.* **2000**, *122*, 2621. (f) Zhan, C.-G.; Landry, D. W. *J. Phys. Chem. A* **2001**, *105*, 1296. (g) Zhan, C.-G.; Zheng, F. *J. Am. Chem. Soc.* **2001**, *123*, 2835.

(42) (a) Zhan, C.-G.; Dixon, D. A. *J. Phys. Chem. A* **2001**, *105*, 11534. (b) Zhan, C.-G.; Dixon, D. A. *J. Phys. Chem. A* **2002**, *106*, 9737. (c) Zhan, C.-G.; Dixon, D. A. *J. Phys. Chem. B* **2003**, *107*, 4403.

(43) Frisch, M. J.; Trucks, G. W.; Schlegel, H. B.; Scuseria, G. E.; Robb, M. A.; Cheeseman, J. R.; Zakrzewski, V. G.; Montgomery, J. A.; Stratmann, R. E.; Burant, J. C.; Dapprich, S.; Millam, J. M.; Daniels, A. D.; Kudin, K. N.; Strain, M. C.; Farkas, O.; Tomasi, J.; Barone, V.; Cossi, M.; Cammi, R.; Mennucci, B.; Pomelli, C.; Adamo, C.; Clifford, S.; Ochterski, J.; Petersson, G. A.; Ayala, P. Y.; Cui, Q.; Morokuma, K.; Malick, D. K.; Rabuck, A. D.; Raghavachari, K.; Foresman, J. B.; Cioslowski, J.; Ortiz, J. V.; Stefanov, B. B.; Liu, G.; Liashenko, A.; Piskorz, P.; Komaromi, I.; Gomperts, R.; Martin, R. L.; Fox, D. J.; Keith, T.; Al-Laham, M. A.; Peng, C. Y.; Nanayakkara, A.; Gonzalez, C.; Challacombe, M.; Gill, P. M. W.; Johnson, B.; Chen, W.; Wong, M. W.; Andres, J. L.; Gonzalez, A. C.; Head-Gordon, M.; Replogle, E. S.; Pople, J. A. *Gaussian 98*, Revision A.6; Gaussian, Inc.: Pittsburgh, PA, 1998.

(44) Cancès, E.; Mennucci, B. *J. Chem. Phys.* **2001**, *114*, 4744.

(45) Cossi, M.; Rega, N.; Scalmani, G.; Barone, V. *J. Chem. Phys.* **2001**, *114*, 5691.

(46) Cances, M. T.; Mennucci, B.; Tomasi, J. *J. Chem. Phys.* **1997**, *107*, 3032.

(47) Cossi, M.; Barone, V.; Mennucci, B.; Tomasi, J. *Chem. Phys. Lett.* **1998**, *286*, 253.

(48) Mennucci, B.; Cammi, R.; Tomasi, J. *J. Chem. Phys.* **1998**, *109*, 2798.

(49) Chipman, D. M. *J. Chem. Phys.* **2002**, *116*, 10129.

(50) Barone, V.; Cossi, M.; Tomasi, J. *J. Chem. Phys.* **1997**, *107*, 3210.

(51) Frisch, M. J.; Trucks, G. W.; Schlegel, H. B.; Scuseria, G. E.; Robb, M. A.; Cheeseman, J. R.; Montgomery, J. A., Jr.; Vreven, T.; Kudin, K. N.; Burant, J. C.; Millam, J. M.; Iyengar, S. S.; Tomasi, J.; Barone, V.; Mennucci, B.; Cossi, M.; Scalmani, G.; Rega, N.; Petersson, G. A.; Nakatsuji, H.; Hada, M.; Ehara, M.; Toyota, K.; Fukuda, R.; Hasegawa, J.; Ishida, M.; Nakajima, T.; Honda, Y.; Kitao, O.; Nakai, H.; Klene, M.; Li, X.; Knox, J. E.; Hratchian, H. P.; Cross, J. B.; Adamo, C.; Jaramillo, J.; Gomperts, R.; Stratmann, R. E.; Yazyev, O.; Austin, A. J.; Cammi, R.; Pomelli, C.; Ochterski, J. W.; Ayala, P. Y.; Morokuma, K.; Voth, G. A.; Salvador, P.; Dannenberg, J. J.; Zakrzewski, V. G.; Dapprich, S.; Daniels, A. D.; Strain, M. C.; Farkas, O.; Malick, D. K.; Rabuck, A. D.; Raghavachari, K.; Foresman, J. B.; Ortiz, J. V.; Cui, Q.; Baboul, A. G.; Clifford, S.; Cioslowski, J.; Stefanov, B. B.; Liu, G.; Liashenko, A.; Piskorz, P.; Komaromi, I.; Martin, R. L.; Fox, D. J.; Keith, T.; Al-Laham, M. A.; Peng, C. Y.; Nanayakkara, A.; Challacombe, M.; Gill, P. M. W.; Johnson, B.; Chen, W.; Wong, M. W.; Gonzalez, C.; Pople, J. A. *Gaussian 03*, Revision A.1; Gaussian, Inc.: Pittsburgh, PA, 2003.

(52) Tissandier, M. D.; Cowen, K. A.; Feng, W. Y.; Gundlach, E.; Cohen, M. H.; Earhart, A. D.; Coe, J. V. *J. Phys. Chem. A* **1998**, *102*, 7787.

(53) Tawa, G. J.; Topol, I. A.; Burt, S. K.; Caldwell, R. A.; Rashin, A. A. *J. Chem. Phys.* **1998**, *109*, 4852.

(54) McDouall, J. J.; Peasley, K.; Robb, M. A. *Chem. Phys. Lett.* **1988**, *148*, 183.

(55) Atkins, P. W. *Physical Chemistry*, 3rd. ed.; Oxford University Press: New York, 1988; p 432.

(56) Kotz, J. C.; Purcell, K. F. *Chemistry & Chemical Reactivity*; CBS College Publishing: New York, 1987; p 977.